Lab on a Chip

Cite this: *Lab Chip*, 2011, **11**, 4181

www.rsc.org/loc

PAPER

Microfluidic Wheatstone bridge for rapid sample analysis†

Melikhan Tanyeri,[a] Mikhil Ranka,[a] Natawan Sittipolkul[a] and Charles M. Schroeder*[ab]

Received 6th July 2011, Accepted 28th September 2011
DOI: 10.1039/c1lc20604d

We developed a microfluidic analogue of the classic Wheatstone bridge circuit for automated, real-time sampling of solutions in a flow-through device format. We demonstrate precise control of flow rate and flow direction in the "bridge" microchannel using an on-chip membrane valve, which functions as an integrated "variable resistor". We implement an automated feedback control mechanism in order to dynamically adjust valve opening, thereby manipulating the pressure drop across the bridge and precisely controlling fluid flow in the bridge channel. At a critical valve opening, the flow in the bridge channel can be completely stopped by balancing the flow resistances in the Wheatstone bridge device, which facilitates rapid, on-demand fluid sampling in the bridge channel. In this article, we present the underlying mechanism for device operation and report key design parameters that determine device performance. Overall, the microfluidic Wheatstone bridge represents a new and versatile method for on-chip flow control and sample manipulation.

Introduction

Lab-on-a-chip microfluidic systems offer several advantages for applications involving sample analysis and small-scale synthesis, including reduced amounts of reagents and miniaturized instrumentation.[1,2] Microfluidic devices allow for on-chip integration of multiple process modules for synthesis and analysis, including reactors, mixers, separators and detectors. Incorporation of real-time sampling and monitoring schemes allows for robust control of integrated chemical processes. In this way, rapid sampling of media or suspended particles, cells or droplets enables efficient process monitoring and provides insight into fundamental chemical and biological phenomena.[3–8]

Flow control is an essential component of microfluidic systems. A number of flow manipulation and control methods based on pressure-driven[9–18] and electroosmotic[18–21] flow have been recently developed. A major challenge in pressure-driven microfluidic systems is rapid and precise generation and manipulation of steady flows with sufficient temporal response and reproducibility. Device performance is often hampered by a lack of precise and reproducible control of absolute pressure at the device inlet,[10–14] especially when an external pressure source such as a gas tank, a syringe and/or a peristaltic pump is utilized. Furthermore, interfacial pressure drops in reservoirs within microdevices present a challenge in generating reproducible, steady flows in microfluidic systems, and current strategies for flow generation generally lack the ability to reverse flow direction while retaining precision and reproducibility.

Microfluidic systems are useful platforms for integrated analysis of particles or reagents. In-line assays for monitoring particles, cells or droplets are typically performed by: i) splitting and diverting a small plug of fluid from the main sample stream[22] or ii) passively isolating particles from the main stream using physical barriers such as wells or pockets.[23–27] Although these methods are straightforward, current approaches may be limited by sample loss and an inability to manipulate or re-direct isolated samples. From this perspective, development of new sampling methods allowing for in-line monitoring of continuous flow processes would enable rapid and efficient "on-chip" sample analysis.

Here, we present a microfluidic device that enables rapid and precise manipulation of steady flows within a microfluidic channel. Overall, the device is a microfluidic analogue of a Wheatstone bridge, which is a classic electrical circuit used to measure resistance (Fig. 1). The device allows for fine-scale control of flow rate and flow direction by using a single on-chip metering valve. In this way, flow direction in a microchannel can be switched independently of the external pressure at the device inlet. In this device, an on-chip membrane valve located in one of the microchannels functions as the "variable resistor", such that the valve opening is continually adjusted in order to manipulate the pressure drop and actively control both the flow rate and flow direction within the "bridge" microchannel.

In this work, we describe a microfluidic device that allows for control of flow rate and flow direction, while enabling in-line

[a]*Department of Chemical and Biomolecular Engineering, University of Illinois at Urbana-Champaign, 600 S. Mathews Ave, Urbana, IL, 61801, USA. E-mail: cms@illinois.edu; Fax: +1 (217) 333-5052; Tel: +1 (217) 333-3906*
[b]*Center for Biophysics and Computational Biology, University of Illinois at Urbana-Champaign, Urbana, IL, USA*

† Electronic supplementary information (ESI) available: Theoretical analysis of the microfluidic Wheatstone bridge, characterization of the membrane valve, device fabrication and three movies of particle sampling and confinement using the microfluidic Wheatstone bridge. See DOI: 10.1039/c1lc20604d

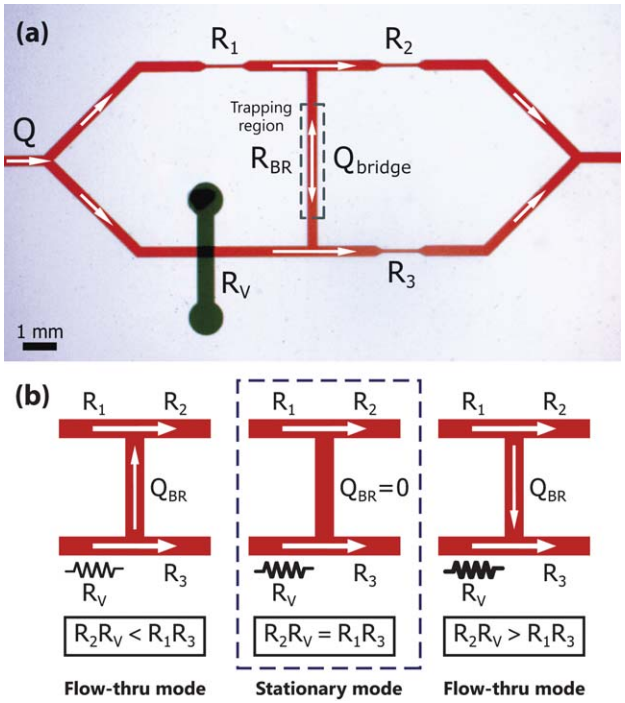

Fig. 1 (a) Optical micrograph of the microfluidic Wheatstone bridge. Two parallel branches (red) from an inlet stream are connected by a perpendicular "bridge" channel. The bridge divides the parallel branches into four segments, each with a distinct flow resistance (R_1, R_2, R_3, R_V). One segment contains a metering valve (dark green), which functions as a variable resistor (R_V) to control flow within the bridge. (b) Flow control in the Wheatstone bridge. The flow rate and direction of flow in the bridge are controlled by an on-chip metering valve. For $R_2R_V < R_1R_3$, flow is directed towards the upper branch (left panel). Similarly, when $R_2R_V > R_1R_3$, flow is directed towards the lower branch (right panel). For $R_2R_V = R_1R_3$, the resistance is balanced, which completely stops the flow within the bridge such that $Q_{bridge} = 0$ (middle panel).

monitoring and rapid sampling in continuous flows. The device functions as an automated dynamic sampler with fine-scale control of fluid motion within the bridge channel (Fig. 1). In this way, fluid samples can be readily routed or analysed by slowing or completely stopping sample flow within the bridge channel, which circumvents the need to repeatedly halt the continuous flow of the main sample stream at the device inlet. The automated sampling method described in this work is a useful and versatile tool for "on-chip" analysis in microfluidic devices.

In this paper, we report on the design and operation of a microfluidic Wheatstone bridge and demonstrate application for flow control and sample analysis. We discuss the underlying mechanism for device operation, including the role of an integrated, on-chip valve for flow control, and effective sample isolation and confinement. Finally, we show proof-of-principle device operation by confining solutions of suspended particles in an "on-demand" format using an automated control algorithm.

Materials and Methods

Microfluidic Wheatstone bridge

The flow control and manipulation method for sample isolation described in this work is based on a microfluidic analogue of the Wheatstone bridge (Fig. 1a). Two parallel branches of a sample stream (shown in red) are connected by a perpendicular "bridge" channel, which divides the parallel streams into four channels. Each of these channels has a distinct flow resistance (depending on dimensions and geometry), and serves as one of the five resistors (R_1, R_2, R_3, R_V and R_{BR}) in the Wheatstone bridge, as shown in Fig. 1a. The volumetric flow rate in the bridge channel can be expressed in terms of the flow resistances and the total flow rate Q (see ESI†):

$$Q_{bridge} = Q\,\frac{R_1R_3 - R_2R_V}{(R_1+R_V)(R_2+R_3) + R_{BR}(R_1+R_2+R_3+R_V)} \quad (1)$$

One of the channels (Fig. 1a, lower left) contains an on-chip metering valve (shown in dark green), which functions as a variable resistor to control fluid flow in the bridge. At one particular value of valve resistance, the flow in the bridge is balanced such that:

$$R_1R_3 = R_2R_V \quad (2)$$

When eqn (2) is satisfied, the flow potentials at each end of the bridge channel are equal, and there is no flow through the bridge ($Q_{bridge} = 0$). By adjusting the flow resistance (R_V) of the lower branch channel using the on-chip metering valve, the flow within the bridge can be shifted towards either side (Fig. 1b). If $R_1R_3 < R_2R_V$, then the flow at the bridge will be directed toward the lower branch (Fig. 1b). Similarly, if $R_1R_3 > R_2R_V$, then the direction of flow is reversed towards the upper branch. Fine-scale adjustment of the flow resistance using the on-chip valve facilitates precise regulation of the volumetric flow rate in the bridge (Q_{bridge}). In this manner, the flow rate and the direction of flow in the bridge are manipulated by dynamic control of the valve. For instance, if the flow resistances are equal ($R_1 = R_2 = R_3 \equiv R_{BR}$). and R_V can be adjusted within the range $R/5 < R_V < 3R$, then the flow rate at the bridge can be manipulated within the range $-Q/7 < Q_{bridge} < +Q/7$ see ESI†).

The microfluidic Wheatstone bridge consists of a hybrid poly (dimethylsiloxane) (PDMS)/glass microdevice fabricated by standard multilayer soft-lithography techniques (Fig. 1a).[28] The "resistor" units comprising the microfluidic Wheatstone bridge consist of rectangular microchannels with short constrictions in all channels except for the bridge channel. In each resistor unit, the flow resistance depends on the geometry and the dimensions (width w, height h and length L) of the microchannels and constrictions. In our devices, typical channel dimensions for the microchannels are $w = 300$ μm, $h = 30$ μm, $L = 7.5$ mm, and dimensions for the constrictions are $w_C = 100$ μm, $h_C = 30$ μm, $L_C = 1$ mm. Typical dimensions for the bridge channel are $w_{BR} = 100$ μm, $h_{BR} = 30$ μm, $L_{BR} = 3$ mm, and the bridge does not contain a constriction. In this way, these channel dimensions approximately yield equal flow resistances for the fixed (constant) "resistors", such that $R_1 = R_2 = R_3 = R \cong R_{BR}$.

One of the microchannels in the microfluidic Wheatstone bridge contains a metering valve, which is utilized to adjust flow resistance by changing the valve opening. The metering valve is a membrane valve, which consists of a microchannel positioned above the fluidic channel and separated by a thin (30–70 μm) elastomeric (PDMS) membrane. The valve microchannel

typically has a width equal to the channel width w and a valve length $L_V = 0.5$ mm. When the valve is pressurized, the membrane deflects downwards into the fluidic layer, thereby changing the cross-sectional area and flow resistance of the fluidic microchannel positioned beneath the valve. The valve opening (and therefore the cross-sectional area) is inversely proportional to the pressure applied to the membrane[29] (see Fig. S3 in ESI†). By dynamic control of membrane valve pressure, the valve opening is typically regulated within 25–100% of the fully-open state, corresponding to an overall manipulation range of $3R/4 < R_V < 15R/4$ for the flow resistance of the channel. In this manner, adjusting the valve opening allows for regulation of the flow rate in the bridge within $-Q/6 < Q_{bridge} < +Q/30$.

Sampling at the bridge channel

The microfluidic Wheatstone bridge is utilized to isolate samples from a continuously flowing stream for in-line monitoring and analysis. Sampling can be performed in two mutually exclusive modes referred to as "flow-thru" or "stationary" mode (Fig. 1b). In "flow-thru" mode, the bridge is unbalanced, and a fraction of the sample stream flows through the bridge (Fig. 1b, left and right panels). In this mode, the bulk velocity of the sample stream is "slowed down" in the bridge channel, such that the sample flow rate in the bridge is adjusted to a small fraction of the total flow rate by controlling the metering valve according to eqn (1). In "stationary" mode, the bridge is balanced precisely by adjusting the valve to satisfy eqn (2), and flow in the bridge is completely stopped (Fig. 1b middle panel). When operating in stationary mode, a small portion of the sample stream can be effectively confined at the bridge for examination and analysis.

Results and discussion

Demonstration of "on-demand" sample analysis and device characterization

As a proof-of-principle demonstration of device function, we performed dynamic sampling of particulate flows using an automated microfluidic Wheatstone bridge (Fig. 2). A feedback control algorithm is used to automate device operation for sample analysis (see below). In these experiments, we study the motion of micron-sized fluorescent beads suspended in aqueous solution, thereby validating the general strategy for in-line sample analysis in a continuous flow format. Here, we analysed aqueous suspensions of 2.2 μm diameter fluorescent polystyrene beads, which are delivered into microfluidic devices using a syringe pump with bulk volumetric flow rates in the range of 10–500 μL h^{-1}. The bridge section of the microfluidic device is imaged at 3.5× or 10× using an inverted microscope (Olympus IX71) equipped with a high numerical aperture objective lens and a CCD camera.

Fig. 2a shows the isolation of solutions containing fluorescent particles in the bridge channel. In these experiments, we operate the device in "stationary mode" such that fluid flow in the bridge channel is completely stopped, which enables long-term observation and analysis of particles (see Movie 1 and Movie 2 in ESI†). In contrast to the well-resolved images of stationary particles confined in the bridge channel, the images of flowing particles in the main stream appear as streaks due to the fast flow rate in the main channel (300 μL h^{-1}), where data was acquired at 30 frames/s. Fig. 2b shows the transient stopping trajectories for nine particles isolated from the main stream and simultaneously confined within the bridge channel (see Movie 3 in ESI†). The average stopping distance is a function of the feedback control algorithm (see Fig. 3c).

In order to elucidate the basic operation principles of the microfluidic Wheatstone bridge, we studied the effect of the membrane valve on modulating fluid flow in the bridge channel (Fig. 3). The membrane valve functions as the variable resistor and is a key component in regulating flow in the bridge channel. We characterized the ratio of flow rate in the bridge to the total flow rate as a function of the membrane valve opening (Fig. 3a). Experimental data (red diamonds) is obtained by adjusting the pressure applied to the membrane valve (0–15 psi) while measuring the flow rate in the bridge channel. Next, the applied pressure is converted to a normalized valve opening using a calibration curve (see ESI†). As shown in Fig. 3a, the experimental data is in good agreement with the theoretical response curve (blue solid line), which is obtained using eqn (1) by calculating the individual flow resistances of each device component (channels, constrictions) in the Wheatstone bridge (see ESI†). The membrane valve is modeled as a constriction inducing uniform height changes along one of the channels.[29] Overall, the response curve has a sigmoidal shape. The bridge is balanced when the membrane valve is 47% open, which results in zero flow in the bridge channel. The flow direction in the bridge channel can be modulated by fine-scale adjustment of the valve around the balance point. Based on the valve response, the flow rate in the bridge channel can be regulated to within $-0.25Q < Q_{bridge} < +0.09Q$, where Q is the total volumetric flow rate. This range of flow rates corresponds to devices with $w_{BR} = 300$ μm, such that the dimensions for all channels on the device are identical. Note that this differs from the range reported in the previous section ($-Q/6 < Q_{bridge} < +Q/30$), which corresponds to devices with $w_{BR} = 100$ μm.

In addition to experiments, we theoretically characterized key device design parameters affecting control of the flow rate in the bridge (see ESI†). Specifically, we determined Q_{bridge}/Q as a function of normalized valve opening. We examined the flow rate ratio Q_{bridge}/Q for several device parameters, including the length and width of the microchannels and constrictions, the length and the width of the bridge microchannel, and the length of the membrane valve. Together, these results provide important guidelines for custom engineering of the Wheatstone bridge for specific applications by tailoring the flow rate response curve (Q_{bridge}/Q as a function of valve opening).

Automated control of the microfluidic Wheatstone bridge

We developed an automated feedback control mechanism to confine fluid streams in the microfluidic Wheatstone bridge. When operated in "stationary mode", an automated feedback controller is used to actively adjust valve opening by dynamic pressurization, which regulates fluid streams for sample analysis. We developed a custom control algorithm (LabVIEW) consisting of the following steps: 1) *image acquisition*: a camera captures an image of the bridge channel, 2) *image processing*: a computer

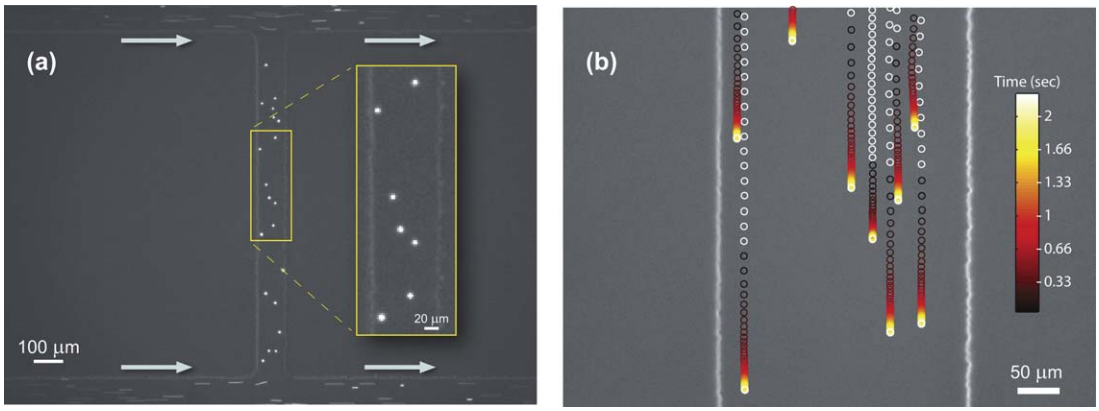

Fig. 2 Particle confinement in the microfluidic Wheatstone bridge. (a) Suspended particles are confined in the bridge channel in a stagnant stream while continuous fluid flow is maintained for the streams in the main channel. Here, fluorescent microspheres (2.2 μm diameter) are sampled from the main stream and effectively trapped within the bridge channel using automated flow control. The total flow rate is Q = 300 μL h^{-1}, and the width and length of the bridge channel are 100 μm and 1 mm, respectively. The channels in the lower and upper branch (channel width, 300 μm) are partially shown. (b) Multiple particles are confined simultaneously when the automated Wheatstone bridge is activated in "stationary" mode. Trajectories of nine particles (2.2 μm fluorescent polystyrene microspheres) trapped simultaneously at the bridge channel are shown. (bridge width, 300 μm) White and colour coded circles show the trajectories of the particles before and after the automated control algorithm is activated, respectively. The scale bar on the right shows the corresponding time scale.

processes the image by tracking and localizing the center-of-mass positions of suspended particles, 3) *controller logic*: a controller determines the pressure required for the on-chip valve to control fluid flow based on the velocity of the suspended particles, 4) *control implementation*: an electronic pressure regulator applies the updated pressure to the on-chip membrane valve, which ultimately results in adjustment of fluid flow in the device. Using the device in the stationary mode of operation, the valve opening is repeatedly adjusted until the flow resistances in the Wheatstone bridge are balanced, thereby completely stopping the flow in the bridge channel ($Q_{bridge} = 0$).

The microfluidic Wheatstone bridge balance point can be determined by characterizing the flow rate response curve, as shown in Fig. 3a. In one approach, the membrane valve opening can be manually set to the bridge balance point in order to confine sample particles in the bridge (see Movie 1 ESI†). However, the pressure corresponding to the bridge balance point typically shows slight variations between different microdevices or across different experiments due to variability in device fabrication or fluctuations in flow rates, respectively.

To ensure robust control and precise regulation of sample streams, we implement an automated control system for flow control. In particular, we use a linear (proportional) feedback control algorithm to control fluid flow in the bridge channel:

$$P' = P + \kappa \cdot \Delta x \quad (3)$$

where κ is the proportional gain constant, Δx is the distance over which a particle traverses between consecutive frames, and P' and P are the updated and current pressure values, respectively. The feedback control algorithm effectively minimizes the velocity of suspended particles entering a region of interest (see Movie 2 in ESI†). The trapping algorithm is based on monitoring the motion of a single target particle, which is typically either the first particle entering the region of interest or the particle nearest to the center of the region of interest (in the case of multiple particles entering the region of interest simultaneously). Stopping the motion of one particle in the bridge effectively halts the overall fluid flow in the bridge channel. In this way, the automated microfluidic Wheatstone bridge facilitates extended monitoring and analysis of fluid streams or suspended particles. Moreover, the feedback controller allows for "on-demand" particle sampling such that the user can either maintain and analyze particles in the bridge or simply release them by unbalancing the bridge (see Movie 2 in ESI†). The feedback loop is executed at a rate of ~30 Hz, which is sufficient for confinement of sample particles to within ±5 μm over a time scale of 30 s. The Wheatstone bridge corrects for convective fluid motion, but long-term confinement of Brownian particles will be affected by thermal drift.

Finally, we studied the effect of the proportional gain constant κ and total flow rate Q on the transient response of particle confinement (Fig. 3b–c). Specifically, we measured stopping distances for particles positioned near the vertical centerline in the bridge channel. Stopping distances are measured for several proportional gain values at three different flow rates (Fig. 3b). For a given flow rate and proportional gain value, we obtained consistent results for stopping distances over several trials. At a constant flow rate Q, stopping distance rapidly decreases with increasing proportional gain values. At a constant proportional gain κ, increasing flow rates yields shorter stopping distances, which is a direct consequence of the proportional controller relation in eqn (3). Proportional control implies that larger pressure changes ΔP will be applied for particles traveling at a higher velocity (larger Δx), which results in a more rapid response. Fig. 3c shows time traces of particle positions at five different proportional gain values at a total flow rate Q_{total} = 150 μL h^{-1}. In agreement with results shown in Fig. 3b, stopping distance decreases with increasing proportional gain values. In all cases, the particles are confined within a timescale of 900 msec. At large values of the proportional gain (*e.g.*, $\kappa = 0.020$), particles tend to overshoot their equilibrium position, exhibiting a damped oscillatory trajectory prior to confinement. For even

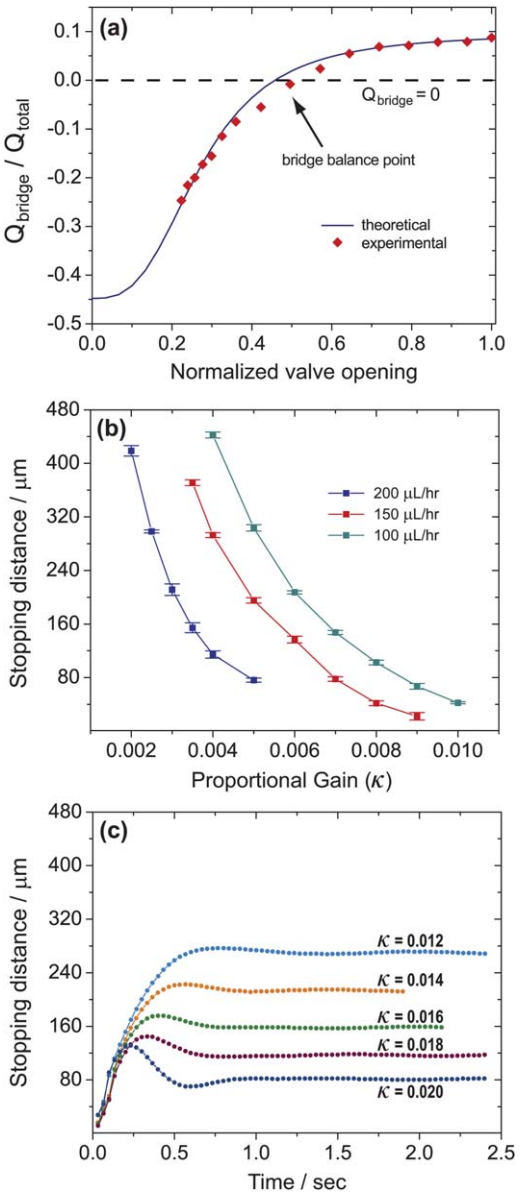

Fig. 3 Characterization of the microfluidic Wheatstone bridge. (a) Response of the flow rate in the bridge channel Q_{bridge} (normalized to total flow rate Q) as a function of membrane valve opening. Experimental data (red diamonds) and theoretical calculations (blue solid line) reveal that the bridge balance point is obtained around ~47% valve opening. Under these conditions, the flow rate at the bridge can be manipulated within $-0.25Q < Q_{bridge} < +0.09Q$. The error bars for the experimental data are on the order of the size of the data points and are provided in ESI†. (b) Effect of the proportional gain constant (κ) on the particle stopping distance at three different flow rates (Q). (c) Effect of the proportional gain constant (κ) on the particle stopping distance at a fixed flow rate (Q).

larger values of the gain ($\kappa > 0.020$), we observed periodic oscillations of trapped particle position, indicating unstable control (not shown).

Conclusions

In this work, we report an integrated microfluidic device that enables rapid and precise manipulation of steady flows within a microchannel. Flow rate and flow direction are manipulated by using a single "on-chip" metering valve. We demonstrate direct application of the device for rapid sampling and confinement of suspended particles in aqueous solutions. The fundamental operating principles of the microfluidic device are analogous to the classic electrical Wheatstone bridge circuit, where bridge current is set to zero by adjusting a variable resistor. As described in this work, the microfluidic Wheatstone bridge generates a stagnant region of fluid within the bridge channel by adjusting flow resistances using an on-chip metering valve. We characterized the effect of valve operation on balancing the bridge, and provided the device design parameters for optimal sampling performance.

Recently, we reported a new flow-based method for particle confinement in a microfluidic device called a hydrodynamic trap.[29,30] The hydrodynamic trap enables high-precision trapping and manipulation of single micro- and nanoscale particles in free-solution. In contrast to the hydrodynamic trap, the microfluidic Wheatstone bridge confines multiple particles simultaneously, albeit without the ability for high-precision manipulation. In the Wheatstone bridge device, "confined" particles are free to diffuse in the bridge channel.

The automated microfluidic Wheatstone device enables fine-scale control and manipulation of flow within a microfluidic channel. Moreover, the device facilitates "on-demand" and real-time sampling of solutions or suspended particles in a continuous flow format without stopping or diverting the main sample stream. The flow rate at the bridge channel can be set to zero or simply reduced to a small fraction of the total flow rate, thereby enabling comprehensive monitoring and analysis of sample particles even in applications requiring high flow rates. In this work, we demonstrate confinement of fluorescent beads, though we anticipate that this method can be readily extended to confine droplets or cells suspended in growth media for analysis.

The method presented in this work can be interfaced with applications requiring downstream processing of samples. For example, solutions or particulates confined in the bridge channel can be diverted into a collection chamber for further on-chip analysis or off-chip processing. In addition, we anticipate that the microfluidic Wheatstone bridge could be used for automated particle sorting, wherein particles matching a pre-defined set of selection criteria (morphology, size, *etc.*) could be identified by custom pattern recognition or computational algorithms and subsequently confined at the bridge for further analysis. Finally, the microfluidic Wheatstone bridge is also amenable to multiplexed applications. A microfluidic device featuring a parallel array of independently controlled bridges would facilitate simultaneous sampling and monitoring of particles from multiple sample streams. Alternatively, an array of bridges positioned in series along a particular sample stream would permit sampling at regular time intervals under continuous flow conditions, which could be used to quantitatively analyse a kinetic process.

Overall, the microfluidic Wheatstone bridge provides a useful alternative to current sampling techniques based on physical barriers or flow networks that divert main sample streams in microdevices. From this perspective, the microfluidic Wheatstone bridge has the potential to enable new analysis techniques in biotechnology, analytical chemistry and materials science. Finally, the microfluidic Wheatstone bridge can serve as

a building block for on-chip fluid control. A number of microfluidic devices have been recently developed based on electrical circuit analogues.[15,16,31–35] In this way, the Wheatstone bridge device could be implemented as a basic logic unit[36] for flow control, wherein the direction of fluid flow at the bridge channel encodes for the two states of a binary digit.

Acknowledgements

We thank Paul J. A. Kenis for providing access to cleanroom facilities for microdevice fabrication. This work was funded by an NIH Pathway to Independence (PI) Award, under Grant No. 4R00HG004183-03.

Notes and references

1 D. R. Reyes, D. Iossifidis, P. A. Auroux and A. Manz, *Anal. Chem.*, 2002, **74**, 2623–2636.
2 P. A. Auroux, D. Iossifidis, D. R. Reyes and A. Manz, *Anal. Chem.*, 2002, **74**, 2637–2652.
3 S. Nagrath, L. V. Sequist, S. Maheswaran, D. W. Bell, D. Irimia, L. Ulkus, M. R. Smith, E. L. Kwak, S. Digumarthy, A. Muzikansky, P. Ryan, U. J. Balis, R. G. Tompkins, D. A. Haber and M. Toner, *Nature*, 2007, **450**, 1235–U1210.
4 J. Hong, J. B. Edel and A. J. deMello, *Drug Discovery Today*, 2009, **14**, 134–146.
5 S. Lindstrom and H. Andersson-Svahn, *Lab Chip*, 2010, **10**, 3363–3372.
6 C. E. Sims and N. L. Allbritton, *Lab Chip*, 2007, **7**, 423–440.
7 W. Wang, C. Yang and C. M. Li, *Lab Chip*, 2009, **9**, 1504–1506.
8 W. Shi, J. Qin, N. Ye and B. Lin, *Lab Chip*, 2008, **8**, 1432–1435.
9 S. Shoji and K. Kawai, *Top. Curr. Chem.*, 2011, **304**, 1–25.
10 L. Saias, J. Autebert, L. Malaquin and J.-L. Viovy, *Lab Chip*, 2011, **11**, 822–832.
11 K. W. Bong, S. C. Chapin, D. C. Pregibon, D. Baah, T. M. Floyd-Smith and P. S. Doyle, *Lab Chip*, 2011, **11**, 743–747.
12 Y. Kim, B. Kuczenski, P. R. LeDuc and W. C. Messner, *Lab Chip*, 2009, **9**, 2603–2609.
13 T. Braschler, L. Metref, R. Zvitov-Marabi, H. van Lintel, N. Demierre, J. Theytaz and P. Renaud, *Lab Chip*, 2007, **7**, 420–422.
14 C. Futterer, N. Minc, V. Bormuth, J. H. Codarbox, P. Laval, J. Rossier and J. L. Viovy, *Lab Chip*, 2004, **4**, 351–356.
15 B. Mosadegh, C.-H. Kuo, Y.-C. Tung, Y.-s. Torisawa, T. Bersano-Begey, H. Tavana and S. Takayama, *Nat. Phys.*, 2010, **6**, 433–437.
16 D. C. Leslie, C. J. Easley, E. Seker, J. M. Karlinsey, M. Utz, M. R. Begley and J. P. Landers, *Nat. Phys.*, 2009, **5**, 231–235.
17 M. Richter, P. Woias and D. Weiss, *Sens. Actuators, A*, 1997, **62**, 480–483.
18 A. Ajdari, *Cr Phys*, 2004, **5**, 539–546.
19 D. J. Beebe, J. Moorthy, C. Khoury and J. S. Moore, *Sens. Actuators, B*, 2001, **75**, 223–229.
20 S. L. R. Barker, D. Ross, M. J. Tarlov, M. Gaitan and L. E. Locascio, *Anal. Chem.*, 2000, **72**, 5925–5929.
21 A. van den Berg, R. B. M. Schasfoort, S. Schlautmann and L. Hendrikse, *Science*, 1999, **286**, 942–945.
22 S.-H. Chen, Y.-H. Lin, L.-Y. Wang, C.-C. Lin and G.-B. Lee, *Anal. Chem.*, 2002, **74**, 5146–5153.
23 J. R. Rettig and A. Folch, *Anal. Chem.*, 2005, **77**, 5628–5634.
24 D. Di Carlo, L. Y. Wu and L. P. Lee, *Lab Chip*, 2006, **6**, 1445–1449.
25 A. M. Skelley, O. Kirak, H. Suh, R. Jaenisch and J. Voldman, *Nat. Methods*, 2009, **6**, 147–152.
26 W.-H. Tan and S. Takeuchi, *Proc. Natl. Acad. Sci. U. S. A.*, 2007, **104**, 1146–1151.
27 J. Nilsson, M. Evander, B. Hammarström and T. Laurell, *Anal. Chim. Acta*, 2009, **649**, 141–157.
28 M. A. Unger, H. P. Chou, T. Thorsen, A. Scherer and S. R. Quake, *Science*, 2000, **288**, 113–116.
29 M. Tanyeri, M. Ranka, N. Sittipolkul and C. M. Schroeder, *Lab Chip*, 2011, **11**, 1786–1794.
30 M. Tanyeri, E. M. Johnson-Chavarria and C. M. Schroeder, *Appl. Phys. Lett.*, 2010, **96**, 224101–224103.
31 A. Plecis and Y. Chen, *Anal. Chem.*, 2008, **80**, 3736–3742.
32 R. Safavieh, G. Z. Zhou and D. Juncker, *Lab Chip*, 2011, **11**, 2618–2624.
33 M. W. Toepke, V. V. Abhyankar and D. J. Beebe, *Lab Chip*, 2007, **7**, 1449–1453.
34 E. W. Lam, G. A. Cooksey, B. A. Finlayson and A. Folch, *Appl. Phys. Lett.*, 2006, **89**, 164105–164103.
35 A. Groisman and S. R. Quake, *Phys. Rev. Lett.*, 2004, **92**, 094501.
36 W. Song and D. Psaltis, *Lab Chip*, 2011, **11**, 2397–2402.

